Numerical Methods in Multidimensional Shocked Flows

SAMUEL Z. BURSTEIN*
Courant Institute of Mathematical Sciences, New York, N. Y.

Numerical methods are described for the calculation of two-dimensional time-dependent inviscid flows that contain shocks. Methods are employed which do not consider the shock as in interior moving boundary. The conservation equations describing such flows are differenced by the Lax-Wendroff method. These procedures allow the computed shock-wave transition to be given over two to three mesh widths while accurately giving the proper jump conditions across the discontinuity. Several additional methods are tested and compared. Numerical results are given for oblique and Mach reflections in air. Comparison with the exact solution for ordinary reflection is good. The Mach reflection calculation agrees with experimental photographic data obtained from wind-tunnel tests.

Introduction

MULTIDIMENSIONAL time-dependent inviscid flows provide a formidable task for computation. The problem is made more difficult by the spontaneous appearance of discontinuities in the fluid. As a result, the partial differential equations, usually written in characteristic form, cannot be integrated over the entire region of space. Instead, one applies the integral form of the differential equations at the discontinuities while continuing to use the differential equations in the remaining regions. Such methods, although conceptually simple, prove lengthy and cumbersome in practice. The purpose of this paper is to introduce the reader to new methods useful in the solution of such problems.

Until most recently, the equations of motion were written in Eulerian or Lagrangian form and then differenced for use in computations. Peter Lax[1-4] suggested that the partial differential equations be written in conservation or divergence free form, and then from these equations the difference equations should be generated. In this paper, this method is tested together with several additional numerical techniques. Although these methods have been applied to flows that are physically steady in time, in general they may be applied to time-dependent problems. The test cases of ordinary oblique shock reflection and Mach reflection were generated as time-dependent problems. This allows the partial differential equations to remain hyperbolic even when the flow is of a mixed type containing subsonic as well as supersonic regions. The solution to these steady problems is obtained asymptotically as $t \to \infty$.

Differential Equations

The mass, momentum, and energy of a fluid contained in a volume region of space will undergo a time rate of change that depends on the flux of such quantities into the space. The inviscid equations of fluid motion may be written so as to fulfill this conservation law

$$\begin{aligned}
\rho_{,t} &= -m_{,x} - n_{,y} \\
m_{,t} &= -\left(p + \frac{m^2}{\rho}\right)_{,x} - \left(\frac{mn}{\rho}\right)_{,y} \\
n_{,t} &= -\left(\frac{nm}{\rho}\right)_{,x} - \left(p + \frac{n^2}{\rho}\right)_{,y} \\
E_{,t} &= -\left[\frac{m}{\rho}(p + E)\right]_{,x} - \left[\frac{n}{\rho}(p + E)\right]_{,y}
\end{aligned} \tag{1}$$

These equations are said to be in divergence free form. Here ρ is the mass per unit volume, the density, and $m = \rho u$ and $n = \rho v$ is the momenta per unit volume in the x and y directions. If e is the specific internal energy and u and v are the velocity components corresponding to their respective momenta, then $E = \rho[e + \frac{1}{2}(u^2 + v^2)]$ is the total energy per unit volume. The subscripts following the comma denote partial differentiation. The pressure p, the fifth dependent variable, may be expressed in terms of the other quantities through the equation of state $p = P(\rho, e)$. If γ is the ratio of specific heats, the functional P can be given by the ideal gas law:

$$p = \rho(\gamma - 1)e = (\gamma - 1)\{E - \tfrac{1}{2}[(m^2 + n^2)/\rho]\}$$

Equation (1) can now be written completely in terms of the conservation variables ρ, m, n, and E. These equations may be written in a more easily handled form. If a vector quantity w has the four components,

$$w = \begin{pmatrix} \rho \\ m \\ n \\ E \end{pmatrix}$$

the conservation law can be expressed as

$$w_{,t} = f_{,x} + g_{,y} \tag{2}$$

The vectors f and g are just functions of w and are given by

$$(w) = \begin{bmatrix} -m \\ \dfrac{\gamma - 3}{2}\dfrac{m^2}{\rho} - (\gamma - 1)E + \dfrac{\gamma - 1}{2}\dfrac{n^2}{\rho} \\ -\dfrac{mn}{\rho} \\ -\gamma\dfrac{Em}{\rho} - \dfrac{\gamma - 1}{2}\dfrac{m^3 + mn^2}{\rho^2} \end{bmatrix}$$

Presented as Preprint 64-2 at the AIAA Aerospace Sciences Meeting, New York, January 20-22, 1964; revision received August 3, 1964. The work presented in this paper is supported by the Atomic Energy Commission Computing and Applied Mathematics Center, Courant Institute of Mathematical Sciences, New York University, under Contract AT(30-1)-1480 with the U. S. Atomic Energy Commission. The author would like to thank Robert Richtmyer for stimulation given[5] as well as Herbert Keller and John Gary for their helpful discussions. Appreciation and thanks is given to Peter Lax for his many ideas, all of which made this paper possible.

* Associate Research Scientist. Member AIAA.

$$g(w) = \begin{bmatrix} -n \\ -\dfrac{nm}{\rho} \\ \dfrac{\gamma-3}{2}\dfrac{n^2}{\rho} - (\gamma-1)E + \dfrac{\gamma-1}{2}\dfrac{m^2}{\rho} \\ -\gamma\dfrac{En}{\rho} - \dfrac{\gamma-1}{2}\dfrac{n^3+nm^2}{\rho^2} \end{bmatrix}$$

Because of the nonlinearity of Eq. (2), smooth solutions, in general, will not exist for all time. If we admit discontinuities in the solution, then the solution of Eq. (2) is a weak solution.[2, 3] A classical solution to a fluid dynamic problem consists of the description of w up to a time when shocks first appear in the domain of interest. A weak solution is a solution that may be continued so as to predict the shocked region for all subsequent times. This is possible since the Rankine-Hugoniot shock conditions, which express conservation of mass, momentum, and energy, are contained in a weak solution. Most important, the weak solutions obtained from a given set of equations is determined by the form in which the equations are written. If new variables z are introduced as nonlinear functions of w such that a conservation law can be written for z, the weak solutions obtained from Eq. (2), say w', can be transformed by these nonlinear functions into a solution z'. In general, z' will not be a weak solution of its own conservation equations.

As a consequence of the theory of weak solutions, the shock is not considered an interior boundary but is a part of the solution,[6] and as such differs from the usual treatment of flows that contain such discontinuities. Usually the shock wave, which is considered as an interior boundary, is located by intersecting characteristics of the same family. At this point, the conditions needed to match the flow on either side are the Rankine-Hugoniot equations.[7] The use of the characteristic equations may then be continued in the smooth part of the flow. The basic difference equations corresponding to Eq. (2) will now be given.

Lax-Wendroff Difference Equations

The Lax-Wendroff method[3, 4] is based on the Taylor expansion of the vector function $w(x, y, t + \Delta t)$ so as to include the second-order term $\frac{1}{2}\Delta t^2 w_{,tt}$. It is this term that, when added to the "intuitive" difference analog of Eq. (2), i.e.,

$$w(x, y, t + \Delta t) = w(x, y, t) + [f_{\hat{x}}(t) + g_{\hat{y}}(t)]\Delta t \quad (3)$$

produces a stable difference approximation. It is a well-known fact that difference equation (3) is unconditionally unstable. However, the central difference approximation could be replaced by a forward or backward difference resulting in a difference scheme that is conditionally stable, but only accurate to $0(\Delta t^2)$. The notation $f_{\hat{x}}$ denotes the centered difference quotient that approximates the derivative $f_{,x}$ within an error that is $0(\Delta x^3)$. This second-order term also increases the order of the accuracy since the truncation error becomes $0(\Delta t^3)$. Lax and Wendroff observed that the form of this added second-order term may be established by the differential equation itself, i.e.,

$$\begin{aligned} \tfrac{1}{2}\Delta t^2 w_{,tt} &= \tfrac{1}{2}\Delta t^2 (f_{,x} + g_{,y})_{,t} = \tfrac{1}{2}\Delta t^2 (f_{,tx} + g_{,ty}) \\ &= \tfrac{1}{2}\Delta t^2 [(Aw_{,t})_{,x} + (Bw_{,t})_{,y}] \\ &= \tfrac{1}{2}\Delta t^2 \{[A(f_{,x} + g_{,y})]_{,x} + [B(f_{,x} + g_{,y})]_{,y}\} \end{aligned} \quad (4)$$

Here we have used A and B to represent the Jacobians of $f(w)$ and $g(w)$ with respect to w. Taking centered differences of (4) and adding the result to (3) yields

$$\begin{aligned} w(x, y, t + \Delta t) = w(x, y, t) + (f_{\hat{x}} + g_{\hat{y}})\Delta t + \\ \{[A(f_x + g_y)]_{\hat{x}} + [B(f_x + g_y)]_{\hat{y}}\}(\Delta t^2/2) + 0(\Delta t^3) \end{aligned} \quad (5)$$

Since this difference scheme is conditionally stable, a linear analysis[4] allows the computation of the linear stability limit. The time increment Δt and space increments Δx and Δy are related to the flow Mach number $M = (u^2 + v^2)^{1/2}/c$ (c being the local sound speed) by

$$\frac{\Delta t}{\Delta x} \leq \frac{(M+1)^{-1}}{c(8)^{1/2}} \qquad \frac{\Delta t}{\Delta y} \leq \frac{(M+1)^{-1}}{c(8)^{1/2}} \quad (5a)$$

Lax and Wendroff modified Eq. (5) by adding an additional term that is $0(\Delta t^4)$. The term is

$$-\tfrac{1}{8}\Delta t^4 (A^2 + B^2) w_{,xxyy} \quad (6)$$

For this difference scheme, a linear analysis[4] gives, for the restriction on the time step,

$$\begin{aligned} \Delta t/\Delta &\leq (2\lambda)^{1/2} \\ \lambda &= \text{eigenvalue}_{\max}\{A^2 + B^2\}, \ \Delta x = \Delta y = \Delta \end{aligned} \quad (6a)$$

The allowable time step given by Eq. (6a) is greater than that given by Eq. (5a). The large amount of additional computing time required at each mesh point for the evaluation of Eq. (6) is a drawback for this method. All computations carried out in this paper were obtained with difference scheme (5) unless otherwise noted. Although there is no unique way of differencing Eq. (5), the conservation form of differencing will be shown.

A Third Difference Scheme of Second-Order Accuracy

The amplification matrix[9] associated with a given differencing scheme is defined by the relation $V(t + \Delta t) = HV(t)$. Here V is a vector function, which, when operated on by H (the amplification matrix), is mapped into a later time. Repeated applications of H results in V being known at increasing intervals of time, $t + 2\Delta t$, $t + 3\Delta t$, etc. The amplification matrix G_1 and G_1' of the Lax-Wendroff difference schemes can be given after a Fourier transformation [allow $\xi \approx \sin\xi$ and $\xi^2 \approx 2(1 - \cos\xi)$] by

$$G_1(\xi, \eta) = I + i(\xi A + \eta B) - \tfrac{1}{2}(\xi A + \eta B)^2 + 0(\xi^3) \quad (7)$$

$$G_1'(\xi, \eta) = G_1(\xi, \eta) - \tfrac{1}{8}(A^2 + B^2)\xi^2\eta^2 \quad (8)$$

Equation (7) can also be obtained by expanding the amplification matrix of exact solutions of Eq. (2), $e^{i(\xi A + \eta B)}$ for small values of the wave numbers ξ and η. In order to generate additional difference schemes (possibly with less stringent stability requirements), one may try to find an approximation to the exact amplification matrix. The approximation should differ from G_1 only in third- or higher-order terms so as to preserve the second-order accuracy of the scheme. This idea was suggested by G. Strang. It is not difficult to show that

$$e^{i(\xi A + \eta B)} = \frac{e^{i\xi A}\, e^{i\eta B} + e^{i\eta B}\, e^{i\xi A}}{2} + 0(\xi^3) \quad (9)$$

Rewrite the right-hand side of Eq. (9) by expanding each of the matrices in a Taylor series and collect terms. Define the result by G_2, a new amplification matrix:

$$\begin{aligned} G_2 &= I + i(\xi A + \eta B) - \tfrac{1}{2}(\xi A + \eta B)^2 + K \\ K &= \frac{A^2B^2 + B^2A^2}{8}\eta^2\xi^2 - \\ &\quad i\left(\frac{AB^2 + B^2A}{4}\xi\eta^2 + \frac{A^2B + BA^2}{4}\eta\xi^2\right) \end{aligned} \quad (10)$$

Equations (10) and (7) differ only by terms which are $0(\xi^3)$. Clearly the difference scheme associated with Eq. (10) is

also second-order accurate. The additional terms are difference analogs of the differential operators

$$\frac{\Delta t^3}{4}\left\{(AB^2 + B^2A)\frac{\partial^3}{\partial x\partial y^2} + (A^2B + BA^2)\frac{\partial^3}{\partial x^2\partial y}\right\} + \frac{\Delta t^4}{8}(A^2B^2 + B^2A^2)\frac{\partial^4}{\partial x^2\partial y^2} \quad (10a)$$

and will be referred to as a triple viscosity, a stabilizing term. The value of these additional terms lies in the fact that the amplification matrix G_2 may be written in the separated and more easily handled form

$$G_2(\xi, \eta) = [M(\xi)N(\eta) + N(\eta)M(\xi)]/2 \quad (11)$$

The abbreviations $M(\xi) \equiv e^{i\xi A}$ and $N(\eta) \equiv e^{i\eta B}$ have been used. It is a well-known fact of hyperbolic equations that A and B are real. Friedrichs has shown that A and B can be symmetrized. Then $M = M^T = M^*$, i.e., M is equal to its transposed complex conjugate M^* as a result of the following relations:

$$M = I + iA\xi - (A^2\xi^2/2) + 0(\xi^3)$$
$$M^* = I - iA^T\xi - (A^2)^T(\xi^2/2) + 0(\xi^3)$$
$$M^* = I - iA\xi - (A^2\xi^2/2) + 0(\xi^3)$$

Hence M is Hermitian and also $MM^* = I = M^*M$, i.e., the matrices denoted by M (and N) are unitary. A unitary transformation corresponds to a generalized rotation which leaves all vectors unaltered in length.

Using Eq. (11), the inner product (G_2q, q) (q being an arbitrary unit vector) may be formed:

$$2[G_2(\xi, \eta)q, q] = \{[M(\xi)N(\eta) + N(\eta)M(\xi)]q, q\}$$

The unitary property states $[M(\xi)q, q] \leq 1$ and a similar statement can be made for $N(\eta)$. Hence, the amplification matrix, Eq. (11), satisfies the inequality $[G_2(\xi, \eta)q, q] \leq 1$. According to Lax's new stability theorem,[4] this implies that the absolute value of all integer powers of G_2 are bounded and the difference equations are stable if the time and space increments satisfy the eigenvalue inequalities

$$|\lambda_{\max}(A)|\,\Delta t/\Delta x \leq 1 \qquad |\lambda_{\max}(B)|\,\Delta t/\Delta x \leq 1$$

This is the famous Courant-Friedrichs-Lewy condition.[8]

It is clear that the three additional terms represented by K in Eq. (10) act as stabilizers so as to allow the maximum possible time step for these explicit methods. The price one pays is the increase in computation time per net point because of the large number of matrix multiplications.

A Fourth Difference Scheme Using Pseudoviscosity

The idea of introducing an artificial viscosity into shock calculations is attributed to Von Neumann and Richtmyer.[6] They wanted to produce a smooth transition across the shock in all the dependent variables when using the partial differential equations of motion everywhere in the flow field. The idea is to introduce an additional viscous pressure term ϕ wherever the pressure term p appears, i.e., the substitution $p + \phi \rightarrow p$. In vector notation, Eq. (2) becomes

$$w_{,t} = (f + r)_{,x} + (g + s)_{,y} \quad (12)$$

The new vectors are defined by

$$r = \begin{pmatrix} 0 \\ -\phi \\ 0 \\ -(m/\rho)\phi \end{pmatrix} \qquad s = \begin{pmatrix} 0 \\ 0 \\ -\phi \\ -(n/\rho)\phi \end{pmatrix} \quad (13)$$

The value of these vectors should be small when away from sharp compressions and should attain maximum values in the shock region. ϕ should have a nonzero contribution when the shocked flow is locally one-dimensional and should be invariant under a rotation of coordinates. A simple form for the viscosity is

$$\phi = \beta^2\rho[(\partial u/\partial x) + (\partial v/\partial y)]^2$$

This form reduces to the Richtmyer viscosity in one dimension.[9] The constant β has the dimension of length and is proportional to Δx or Δy, and so ϕ has the dimensions of pressure. ϕ is also restricted when the fluid is undergoing a local expansion, i.e.,

$$\left.\begin{aligned} \phi &= \beta^2\rho\left[\left(\frac{m}{\rho}\right)_{,x} + \left(\frac{n}{\rho}\right)_{,y}\right]^2 && \text{if } \left(\frac{m}{\rho}\right)_{,x} < 0, \left(\frac{n}{\rho}\right)_{,y} < 0 \\ &= \beta^2\rho\left[\left(\frac{m}{\rho}\right)_{,x}\right]^2 && \text{if } \left(\frac{n}{\rho}\right)_{,y} \geq 0, \left(\frac{m}{\rho}\right)_{,x} < 0 \\ &= \beta^2\rho\left[\left(\frac{n}{\rho}\right)_{,y}\right]^2 && \text{if } \left(\frac{m}{\rho}\right)_{,x} \geq 0, \left(\frac{n}{\rho}\right)_{,y} < 0 \\ &= 0 && \text{if } \left(\frac{m}{\rho}\right)_{,x} \geq 0, \left(\frac{n}{\rho}\right)_{,y} \geq 0 \end{aligned}\right\} \quad (14)$$

As a result of the dissipation terms, Eq. (12) is no longer a first-order quasilinear partial differential equation. Based on previous experience[9] with the one-dimensional form of these higher-order equations, it is expected that the allowable time increment for stability of the difference analog to Eq. (12) will be appreciably smaller than required for the previous difference schemes.

During computations, β^2 was chosen small enough so that the shock transition would be as sharp as possible, but large enough so that oscillations would be damped. A value of $\beta^2 = 1.9$ seemed to be a good compromise. This value falls within the range obtained by Richtmyer for the one-dimensional case. Since β is proportional to Δx it is possible to neglect the presence of $r_{,x}$ and $s_{,y}$ in the term $w_{,tt}\,\Delta t^2/2$ since third-order quantities are neglected. The proposed difference scheme is then

$$w_{i,j}(\Delta t) = \Psi_{i,j}(0) + [r_{i+1/2,j}(0) - r_{i-1/2,j}(0)]\Delta t/\Delta + (s_{i,j+1/2}(0) - s_{i,j-1/2}(0))\Delta t/\Delta \quad (15)$$

subject to the constraints imposed by Eq. (14), where the terms given on the right-hand side of Eq. (16) are represented by $\Psi_{i,j}(0)$.

Interior and Boundary Net Points

Usually the computations performed with the four difference methods were carried out on a square spatial mesh. The one exception was for the flow field of Ref. 12. Here a rectangular array of points were used ($\Delta x = \frac{7}{6}\Delta y$). If one is given initial data at each mesh point (x_i, y_j) at time $t = 0$, i.e., $\rho(x_i, y_j, 0)$, $m(x_i, y_j, 0)$, $n(x_i, y_j, 0)$, and $E(x_i, y_j, 0)$ then the fundamental difference equation for the evaluation of $w(x_i, y_j, t + \Delta t)$ is

$$w_{i,j}(t + \Delta t) = w_{i,j}(t) + \frac{\Delta t}{2\Delta}[f_{i+1,j}(t) - f_{i-1,j}(t)] + \frac{\Delta t}{2\Delta}[g_{i,j+1}(t) - g_{i,j-1}(t)] + \sum_1^4 (-1)^{l-1}C_l(t)\frac{\Delta t^2}{2\Delta^2} \quad (16)$$

Here equal net spacing $\Delta x = \Delta y = \Delta$ is used and the subscripts (i, j) correspond to the net point with coordinates (x_i, y_j). The vectors C_l are evaluated at $(i + \frac{1}{2}, j)$, $(i - \frac{1}{2}, j)$, $(i, j + \frac{1}{2})$ and $(i, j - \frac{1}{2})$, respectively, i.e.,

$$\begin{aligned} C_1 &= A_{i+1/2,j}\{(f_{i+1,j} - f_{i,j}) + \tfrac{1}{4}(g_{i,j+1} - g_{i,j-1} + g_{i+1,j+1} - g_{i+1,j-1})\} \\ C_2 &= T_{-1}^{(x)}C_1 \\ C_3 &= B_{i,j+1/2}\{\tfrac{1}{4}(f_{i+1,j} - f_{i-1,j} + f_{i+1,j+1} - f_{i-1,j+1}) + (g_{i,j+1} - g_{i,j})\} \\ C_4 &= T_{-1}^{(y)}C_3 \end{aligned} \quad (17)$$

Table 1 Results of numerical stability tests

Method	Experimental stability value
1. Eq. (16)	≤ 0.86 CFL
2. Eq. (16) + Eq. (6)	≤ 0.86 CFL
3. Eq. (9)	≤ 0.8 CFL
4. Eq. (15)	≤ 0.1 CFL

$T_\theta^{(x)}$, $T_\theta^{(y)}$ are translation operators that shift the index of the expressions for C_1 and C_3 from i to $i + \theta$ and j to $j + \theta$, respectively. The coefficient matrices are taken to be $A_{i+1/2,\,j} = \frac{1}{2}(A_{i+1,\,j} + A_{i,\,j})$, etc. It is to be noted that once computation is completed at point (x_i, y_j), if computational sequencing is by points on rows (columns), $C_1 \rightarrow C_2$ for point (x_{i+1}, y_j) [$C_3 \rightarrow C_4$ for point (x_i, y_{j+1})]. Hence, except for regions of the flow near the boundary, these vectors are alternately added to and subtracted from the flow canceling in pairs in the interior region. This result follows as a consequence of conservation differencing and insures the conservation of the mass, momentum, and energy in the interior region.

The same difference equations may be used for mesh points on the boundary of the fluid region. Walls or obstructions in the flow field are represented by a string of net points and are treated as regular interior net points. This may be accomplished if the conservation variables are defined on a virtual line of net points constructed within the solid boundary. These points obtain their values via a reflection principle that images the flow properties near the boundary according to simple rules. The virtual points are only used to generate approximations to partial derivatives for the points defining the boundary. If the boundary is parallel to the x axis ($y = y_j$), as is the upper boundary in this paper, the reflection rule is

$$\rho_{i,\,j+1} = \rho_{i,\,j-1} \qquad m_{i,\,j+1} = m_{i,\,j-1}$$
$$n_{i,\,j+1} = -n_{i,\,j-1} \qquad E_{i,\,j+1} = E_{i,\,j-1}$$

For a boundary parallel to the y axis ($x = x_i$), the rules for the density and total energy are the same, but $m_{i+1,\,j} = -m_{i-1,\,j}$ and $n_{i+1,\,j} = n_{i-1,\,j}$.

For boundaries that are not parallel to either coordinate axis but make some angle α with the horizontal, the construction is somewhat more complicated. Here quadratic interpolation and evaluation of derivatives of the conservation variables with unequal spacing is necessary. For this computation[10] instabilities may occur whenever two points come much closer than a characteristic length equal to $c\Delta t$.[7, 11]

The inflow boundary is prescribed as a known constant state. The conditions describing the outflow boundary is more complicated, since centered differences in the x directions cannot be evaluated in the usual manner. Rather than compute the x direction by centered formulas, left-sided differences are used at this boundary. Wherever Eqs. (16) and (17) contain x differences, extrapolated approximations are used.[10]

Shock Relations

The general form of the integral or jump conditions may be obtained from the differential equations (2). If the left-hand side is integrated over a volume region of space while the left-hand side is integrated over the surface defining this region, the result

$$s[w_i] = [F_i \cdot n] \tag{18}$$

is the Rankine-Hugoniot relations valid for a shock contained in the volume region of space. Here n is the unit normal vector to the discontinuity; F_i represents the vector (f_i, g_i), and s is the normal speed of the discontinuity. $[\lambda]$ indicates the jump in λ. Every weak solution must satisfy these jump conditions across a line of discontinuity. This fact was used to test the two-dimensional numerical method as far as its ability to reproduce one-dimensional shocks. When a stationary one-dimensional shock solution is given as the initial condition, the difference equations were identically satisfied for all times t. The Rankine-Hugoniot conditions, in this case ($s = 0$), is

$$[f] = 0 \tag{18a}$$

i.e., $f_+ = f_-$. The two-dimensional equations reduce to

$$w(x, t + \Delta t) = w(x, t) + f^{\wedge}\,\Delta t + (Af_x)_{\frac{1}{2}}(\Delta t^2/2)$$

Since the shock connects two constant states, the centered second derivative vanishes. Across, the shock equation (18a) is satisfied so that at the shock a centered difference in f (numerically equal to $[f]$) vanishes.

Equations (18), after much algebraic manipulation, may be written in the form of a cubic polynomial for the local tangent of the shock angle σ, i.e.,

$$\tan^3\sigma + c_2 \tan^2\sigma + c_1 \tan\sigma + c_0 = 0 \tag{19}$$

The coefficients are given by

$$c_2 = 2(1 - M^2)/\{\tan\alpha[2 + (\gamma - 1)M^2]\}$$
$$c_1 = [2 + (\gamma + 1)M^2]/[2 + (\gamma - 1)M^2]$$
$$c_0 = 2/\{\tan\alpha[2 + (\gamma - 1)M^2]\}$$

The flow makes an angle α with the horizontal, and the Mach number is M. Since $M > 1$, Descartes' rule of signs allows no more than two positive roots and one negative root. The positive roots correspond to the strong and weak compression shocks, the choice of the solution being dictated

Table 2 Comparison of the four difference methods[a]

Eq. (5)	Eqs. (5) and (6)	Eq. (9)	Eq. (15)	
1.000	1.000	1.000	1.000	
1.000	1.000	1.000	1.000	
1.000	1.000	1.000	1.000	exact density 1.0
1.000	1.000	1.000	1.000	
1.000	1.000	1.000	1.000	
1.000	1.000	1.000	1.000	
1.000	1.000	1.000	1.000	
0.999	1.000	1.000	1.000	
1.000	1.000	1.000	1.000	
1.001	1.001	1.000	1.000	
1.000	1.001	1.000	0.999	
0.998	0.999	1.000	0.999	
0.998	0.998	0.999	1.002	
1.003	1.000	0.997	1.000	
1.007	1.005	1.011	1.000	
0.996	0.993	0.988	0.987	
0.982	0.970	0.986	0.991	
0.964	0.948	0.957	1.068	
0.962	0.975	0.995	1.239	
1.246	1.283	1.199	1.499	exact ← shock position
2.072	2.035	2.097	1.796	
2.509	2.479	2.678	2.042	
2.319	2.356	2.248	2.214	exact density 2.277
2.296	2.308	2.265	2.323	
2.327	2.320	2.338	2.342	
2.318	2.314	2.319	2.306	
2.319	2.317	2.306	2.246	
2.337	2.331	2.347	2.216	
2.334	2.330	2.366	2.220	
2.341	2.337	2.369	2.212	

[a] The density is shown at the upper boundary for the case of oblique reflection, $M_{-\infty} = (u^2 + v^2)^{1/2}/c = 2$.

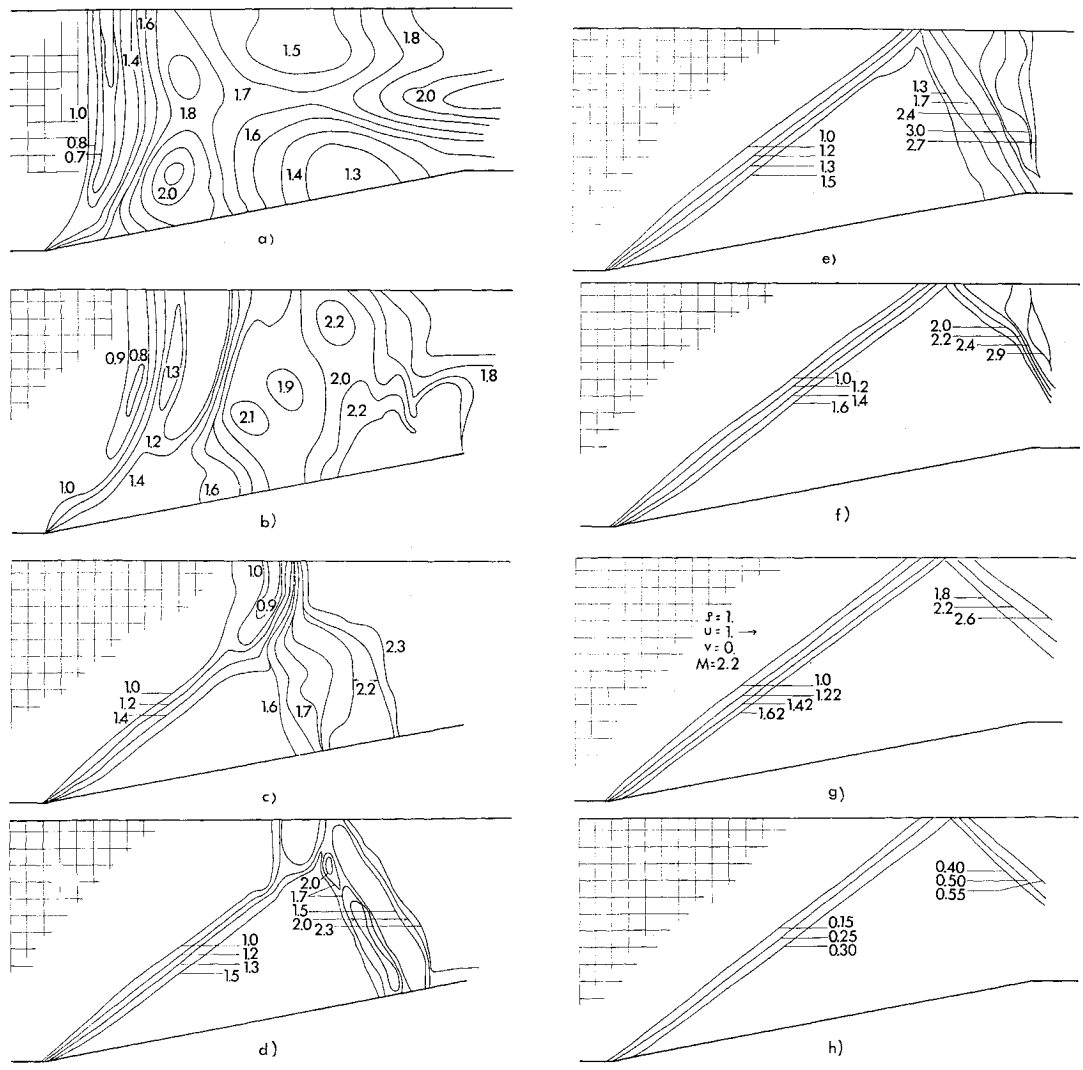

Fig. 1 Approach of the density field to the asymptotic solution for ordinary reflection when $M_{-\infty} = 2.2$ ($\gamma = 1.4$). Figures 1a–1g correspond to the following time multiples of Δt: a) 70; b) 140; c) 210; d) 350; e)420; f) 560; g) 700 ($\Delta t/\Delta = 0.233$). Figure 1h is the pressure field corresponding to 1g. Over-all average density ratio = 2.33, exact = 2.34.

by the boundary condition on the pressure downstream of the shock. An expansion shock corresponds to the negative root, but this leads to a contradiction of the second law of thermodynamics.

Equation (19) together with Eqs. (18) define the flow field for the exact solution of regular oblique shock reflection. Comparison can then be made between exact theory and the solutions generated as a result of the numerical methods. Positive roots are not obtained from Eq. (19) for all values of the parameters M and α. For some range of these parameters, complex roots occur which correspond to the case of Mach reflection. For this case, the flow pattern cannot be predicted exactly and, as a result, the numerical methods must be compared with either approximate theories or experimental evidence.

Initial Conditions

The four difference schemes (16, 16 and 6, 9, and 15) were tested on the problem of ordinary shock reflection. The steady-state solution is such that the flow is everywhere supersonic and irrotational. A constriction or wedge of angle α appears in the channel. In this region, an incident shock changes the flow direction through the angle α so that it is parallel to the wedge. A secondary or reflecting shock from the upper wall changes the flow direction by an equal amount so that it is again parallel to the upper wall. Since these conditions represent an exact solution, it was felt that a comparison of the difference solution of this steady flow problem with the exact solution would be a good measure of the computing methods. Considering the problem as being time-dependent allowed the flow to approach the steady-state shock reflection solution when arbitrary initial data were prescribed. In this way, one could also ascertain the rate of convergence of the method. An incident shock, acting as a strong perturbation on the flow, was set normal to the inflow ($\sigma = \pi/2$) at the toe of the wedge ($x = 0$) whose angle $\alpha = \tan^{-1}(\frac{1}{5})$. The jump conditions across this shock were made to differ from those predicted by the Hugoniot conditions, i.e., if $w_{-\infty}$ is the inflow condition, w_1 is not connected to $w_{-\infty}$ through Eq. (18). In addition, the reflected shock was completely eliminated in the initialization. Then the initial conditions prescribed were

$$\left.\begin{aligned} -\infty < x \leq 0 \\ 0 \leq y \leq y_{\text{wall}} \end{aligned}\right\} w = w_{-\infty}$$
$$\left.\begin{aligned} \infty > x > 0 \\ y_{\text{wedge}} \leq y \leq y_{\text{wall}} \end{aligned}\right\} w = w_1 \qquad (20)$$

For the case of Mach reflection considered in Ref. 12, the initial condition prescribed was that of impulsive flow, i.e., $w(x, y, 0) = w_0$ everywhere. All other cases of Mach reflection used the same conditions as given by Eqs. (20).

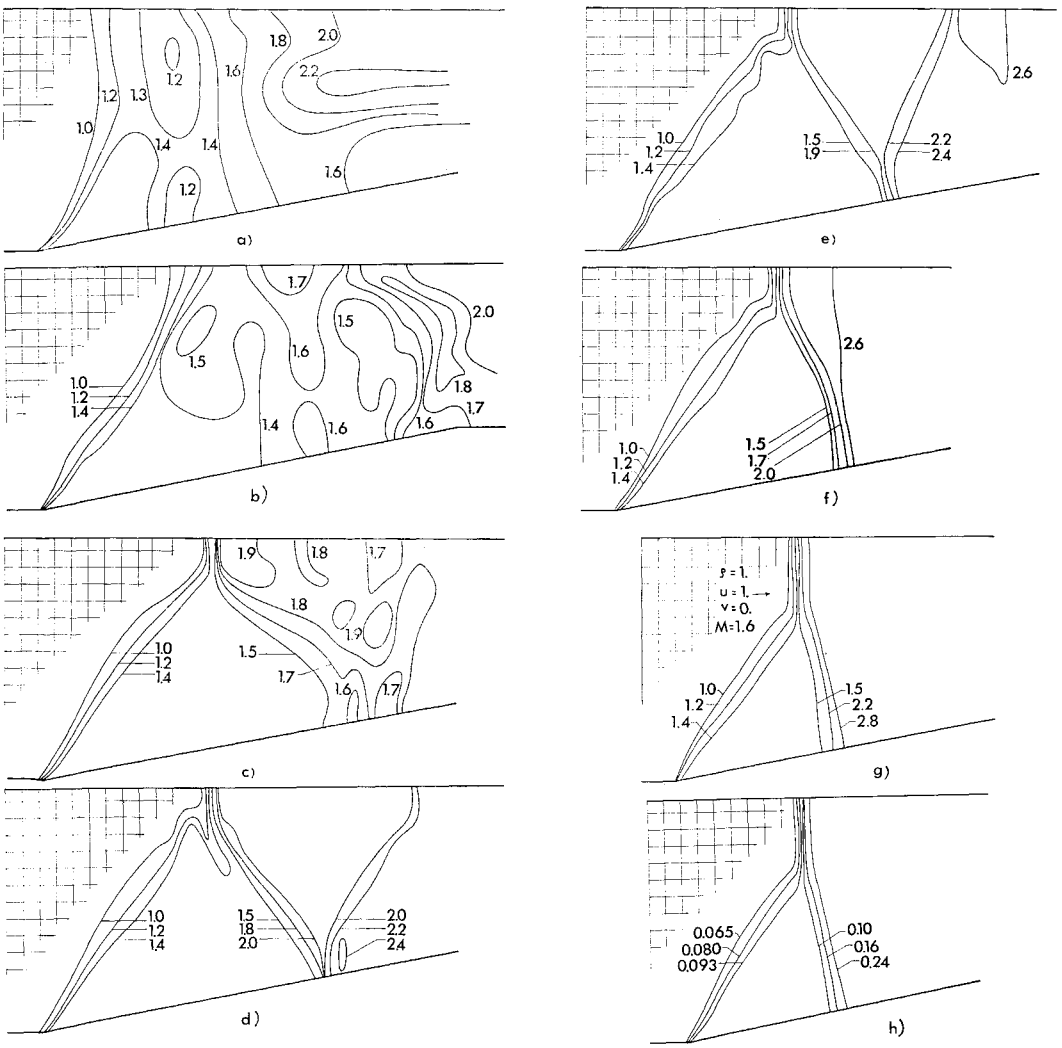

Fig. 2 Approach of the density field to the asymptotic solution for Mach reflection when $M_{-\infty} = 1.6$ ($\gamma = 1.2$). Figures 2a–2g correspond to the following time multiples of Δt: a) 70; b) 140; c) 210; d) 350; e) 420; f) 560; g) 700 ($\Delta t/\Delta = 0.229$). Figure 2h is the pressure field corresponding to 2g.

Tests of Stability and Numerical Results

The Courant-Friedrichs-Lewy (CFL) stability condition $\Delta t/\Delta \leq 1/(|\mathbf{u}| + c) \equiv \text{CFL}$ where $|\mathbf{u}| = (u^2 + v^2)^{1/2}$ was used as a measure of the stability of the difference methods. The difference scheme associated with the triple viscosity should exhibit stability for this value of the time increment. Table 1 gives the empirically obtained values of stability. Method 3 requires a lower value of the time increment compared with the theoretical value. This is probably because the matrices A and B vary quite rapidly in the shocked region, contradicting the assumption of linearization. In addition, the effect of the boundaries and their treatment does not appear in the analysis. Method 2 allows, in practice, a time interval greater than that predicted by Eq. (6a) by a factor of approximately 2. It is clear that the reason for this lies in the stability proof,[4] which makes use of inequality estimates that lead to conservative results.

A comparison of the four methods is shown in Table 2. Notice the spread of the shock at the reflection point on the upper boundary and the resultant decrease in oscillations near the shock position for the method involving Eq. (15). The first three methods seem to give essentially the same result. Since Eq. (16) results in the fastest computation, it was used to give all the following results.

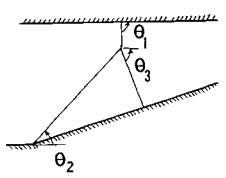

Fig. 3 Geometry of Mach reflection.

This numerical scheme was tested for various values of the Mach number at the inflow boundary, viz., $1.3 \leq M_{-\infty} \leq 3.2$. Exact solutions are compared to the numerical results in Table 3. For the wedge angle used, the flow followed one of two solutions, which are distinct and depend quite strongly on the value of the Mach number. For $M_{-\infty} \leq 1.87$, Mach reflection occurred, whereas for larger values of the Mach number, the asymptotic solution was that of ordinary shock reflection. The methods used were able to predict quite sharply this limiting value of the Mach number. Figure 1 gives the characteristic appearance of the time-dependent solution for values of $M_{-\infty} > 1.87$, whereas Fig. 2 shows the time-dependent Mach reflection solution for $M_{-\infty} = 1.6$ and $\gamma = 1.2$.

These Mach reflection calculations were not compared with experimental data, but the behavior seems to be qualitatively correct. Instead, an additional calculation was performed in which the boundary conditions closely approximated the experimental wind tunnel of Ref. 12. Here $\alpha = \tan^{-1}(\frac{3}{7})$ whereas the spatial mesh was defined by unequal mesh intervals, i.e., $\Delta x = \frac{7}{6}\Delta y$. Quantitative comparison is given at the bottom of Table 4. Here the shock angles are defined by

Table 3 Results of oblique reflection ($\gamma = 1.4$)

$M_{-\infty}$	Wedge angle	Incident shock, deg Computed	Exact	Reflected shock, deg Computed	Exact
2.0	$\tan^{-1}(\frac{1}{5})$	40.2	40.8	45.8	54.0
2.2	$\tan^{-1}(\frac{1}{5})$	37.2	37.2	47.0	46.6
3.0	$\tan^{-1}(\frac{1}{5})$	27.3	28.6	not computed	33.8

Fig. 3. The Mach stem and incident shock angles agree quite well. The reflected shock in the experiment interacted with an expansion fan, and so the agreement here cannot be as good.

A steady-state solution for values of $M_{-\infty} \leq 1.4$, $\alpha = \tan^{-1}(\frac{1}{5})$ could not be obtained. The reason seems to be associated with a combination of factors. The rapidly shrinking triangular region under the triple point combined with the technique of computing derivatives at the surface of the wedge leads to inaccuracies. The reflection method that is used on the wedge is a second-order scheme and hence will be inaccurate when there are large variations in the flow properties, i.e., when many shocks are present in a small region. In addition, for these low values of Mach number, the long Mach shock implies that the flow is basically subsonic in the downstream region, a fact that allows disturbances (which might be generated numerically by the extrapolating procedure) to propagate upstream from that boundary.

In addition, the slipline emerging from the triple point could not be numerically resolved in these calculations. This was probably due to the weakness of the shocks in this study, i.e., the strength of the slipline depends upon the difference of entropy across this discontinuity. The entropy production from a weak shock, however, behaves as the cube of the shock strength.

Table 4 Mach reflection ($\gamma = 1.4$)

$M_{-\infty}$	Wedge angle	Mach stem θ_1, deg	Incident shock θ_2, deg	Reflected shock θ_3, deg
1.85	$\tan^{-1}(\frac{1}{5})$	90.0	46.2	66–80
1.7	$\tan^{-1}(\frac{1}{5})$	90.0	48.7	61–73
1.6	$\tan^{-1}(\frac{1}{5})$	90.0	54.6	65.3
1.5	$\tan^{-1}(\frac{1}{5})$	90.0	59.0	70.2
1.6 ($\gamma = 1.2$)	$\tan^{-1}(\frac{1}{5})$	90.0	52.3	72.4
3.075	$\tan^{-1}(\frac{3}{7})$	90.0	41.0	35.5
	$\Delta x = \frac{7}{6}\Delta y$			
	Experimental[12]			Experimental[12]
3.15	≈23°		40.5–42.5°	≈43.5°

References

[1] Lax, P. D., "Hyperbolic systems of conservation laws II," Commun. Pure Appl. Math. **10**, 537–566 (1957).

[2] Lax, P. D., "Weak solutions of nonlinear hyperbolic equations and their numerical computation," Commun. Pure Appl. Math. **7**, 159–193 (1954).

[3] Lax, P. D. and Wendroff, B., "Systems of conservation laws," Commun. Pure Appl. Math. **13**, 217–237 (1960).

[4] Lax, P. D. and Wendroff, B., "Difference schemes with high order of accuracy for solving hyperbolic equations," NYO Rept. 9759, Courant Institute of Mathematical Sciences, New York Univ. (July 1962).

[5] Richtmyer, R. D., "Proposed fluid dynamics research," unpublished memo., Courant Institute of Mathematical Sciences, New York Univ. (September 28, 1960).

[6] Von Neumann, J. and Richtmyer, R. D., "A method for the numerical calculation of hydrodynamical shocks," J. Appl. Phys. **21**, 232–237 (1950).

[7] Richtmyer, R. D., "Progress report on the Mach reflection calculation," NYO 9764, Courant Institute of Mathematical Sciences, New York Univ. (September 1961).

[8] Courant, R., Friedrichs, K. O., and Lewy, H., "Uber die Partiellen Differenzengleichungen der Mathematischen Physik," Math. Ann. **100**, 32 (1928).

[9] Richtmyer, R. D., *Difference Methods for Initial-Value Problems* (Interscience Publishers, Inc., New York, 1957), Chap. IV.

[10] Burstein, Samuel Z., "Numerical calculations of multidimensional shocked flows," NYO 10,433, Courant Institute of Mathematical Sciences, New York Univ. (November 1963).

[11] Gary, J., private communication (1963).

[12] Gross, R. A. and Chinitz, W., "A study of supersonic combustion," J. Aerospace Sci. **27**, 517–524 (1960).